Globally coupled noisy oscillators with inhomogeneous periodic forcing

Michael Gabbay,[1] Michael L. Larsen,[1] and Lev S. Tsimring[2]
[1]*Information Systems Laboratories, Inc., 10070 Barnes Canyon Road, San Diego, California 92121, USA*
[2]*Institute for Nonlinear Science, University of California, San Diego, La Jolla, California 92093-0402, USA*
(Received 8 June 2004; published 21 December 2004)

We study the collective properties of an array of nonlinear noisy oscillators driven by nonidentical periodic signals. We consider the case of a globally coupled array of harmonically forced, weakly nonlinear oscillators where there is a constant difference between the phases of the forcing signals applied to adjacent oscillators. This system is a prototypical model of a nonlinear phased array receiver. We derive analytical results for the array output in the limit of a large number of oscillators for the noise-free and noisy cases. Numerical simulations show good agreement with the theoretical analysis.

DOI: 10.1103/PhysRevE.70.066212 PACS number(s): 05.45.Xt

I. INTRODUCTION

An ensemble of coupled nonlinear oscillators is a paradigm for many natural processes in physical, chemical, and biological systems as well as in technological devices, such as Josephson junction arrays [1] or solid-state laser arrays [2]. The collective behavior of arrays of nonlinear oscillators has attracted considerable attention in the last two decades. Locally coupled oscillators often exhibit complicated spatiotemporal patterns and chaos [3]. A network of globally coupled oscillators undergoes a phase transition to a synchronized state with nonzero mean-field oscillations [4–9].

The driven dynamics of nonlinear oscillators has a long and rich history. Phenomena of synchronization, parametric resonance, and chaos have been studied in detail. Externally driven networks of coupled oscillators can be utilized for beam steering in phased arrays [10].

Recently, an application of coupled nonlinear oscillators for beam forming in a phased array receiver antenna has been proposed [11,12]. It was shown that locally coupled Van der Pol oscillators demonstrate a superior main-beam resolution and sidelobe suppression compared to their linear counterparts. However, Ref. [12] did not address one of the most important aspects of antenna performance, namely, its behavior in noisy environments. In this paper we investigate the dynamics of an ensemble of nonlinear oscillators driven by external periodic signals and noise. Unlike Ref. [12] we consider an array of *globally* coupled oscillators, as it allows a simpler analytical treatment of the stochastic problem, while not changing the qualitative beam-forming performance of the system. In earlier work [9] a similar problem has been investigated, with the important difference that the periodic driving signal was assumed identical in all elements; thus, the beam-forming abilities of such a network could not be determined. Driven noisy nonlinear oscillators sometimes exhibit the phenomenon of stochastic resonance, which is associated with signal amplification due to noise at a certain optimal noise level [13].

II. GLOBALLY COUPLED OSCILLATOR ARRAY AS A PHASED ARRAY RECEIVER

A conceptual design of an array of globally coupled nonlinear oscillators working as a phased array receiver similar to the one proposed earlier in Ref. [12] is shown in Fig. 1. The N sensor elements H_i are assumed to be equally spaced at a distance d along a straight line. The sensors are driven by external signals $f_j(t)$ that are assumed to differ by a fixed time delay $\Delta T = d \sin\theta/c$, where c is the wave propagation speed and θ is the angle of incidence of the signal with respect to the broadside direction of the array. For a monochromatic plane wave with frequency Ω_s, the time delay translates into phase differences between neighboring elements $\Delta\Phi = \Omega_s \Delta T$. Beam steering, as in conventional phased arrays, can be achieved by insertion of tunable delay elements τ_j. In the following we assume that the beam is steered to the broadside direction, so all $\tau_j = 0$.

For simplicity we assume that the received external signals drive a network of globally coupled weakly nonlinear Van der Pol oscillators that can be described by the following set of coupled Landau-Stuart equations for the complex amplitudes z_j:

$$\dot{z}_j = (G + i\omega_j)z_j - G|z_j|^2 z_j + \frac{\kappa}{N}\sum_{n=1}^{N}(z_n - z_j) + fe^{i(\Omega_s t + \Phi_j)} + \Xi_j, \quad j = 1, \ldots, N, \tag{1}$$

where for an oblique plane wave $\Phi_j = \Delta\Phi(j-1)$ with $\Delta\Phi$ introduced above, G is the oscillator "gain," and Ξ is (complex) stochastic additive white Gaussian noise acting independently on each oscillator. The noise-free behavior of a similar system with nearest-neighbor diffusive coupling and

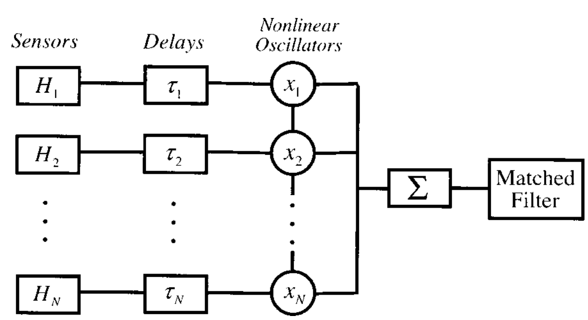

FIG. 1. Nonlinear beam former.

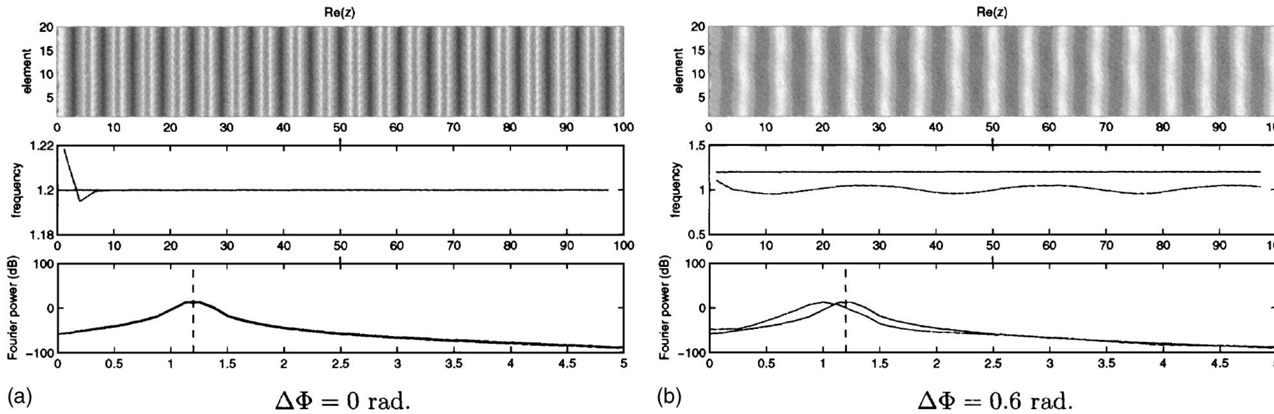

FIG. 2. Comparison of dynamics response of a $N=20$-element array of forced-coupled oscillators. The top panels displays the phase of elements vs time (seconds), the middle panels shows the frequency (radians/second) of the output $y=N^{-1}\sum_{n=1}^{N} z_n$ vs time (seconds), the lower panels compares the spectrum of output (dB) vs frequency (radians/second) with the spectrum of an N-element linear beam former. The synchronized response to a signal incident broadside to the array is visible in (a), whereas in (b) the response is unsynchronized when the forcing signal is incident off-broadside.

identical frequencies was studied in Ref. [12]. For large enough driving strength $f > \Omega_s - \omega$ and small phase differences $\Delta\Phi < \Delta\Phi_c$, the oscillators synchronize to the driving signals, and for larger $\Delta\Phi$ they oscillate on average at their natural frequency ω. This behavior leads to significant differences in the beam pattern, which describes the spatiotemporal response of the output of the network at forcing frequency, of the nonlinear beamformer as compared to a linear one. The noise-free dynamics of the globally coupled array (1) is qualitatively similar. Figure 2 shows the results of numerical simulations of this system with $N=20$ elements for $\omega=1$, $\Omega_s=1.2$, $\kappa=10$, $f=1$, and $G=1$.

III. PHASE APPROXIMATION

For the theoretical analysis of the oscillator array dynamics, we use the standard simplification known as the *phase approximation* [14]. Namely, we introduce $z_j = a_j e^{i(\Omega_s t + \varphi_j)}$ and assume that the magnitudes a_j are slaved to the phases φ_j. This approximation is applicable for large gain $G \gg \kappa$, f, $\Omega_s - \omega$. Furthermore, for large gain G, the amplitudes of all oscillators are close to one. Ignoring the small deviations $a_j - 1$, we obtain the following equation for the phases:

$$\dot{\varphi}_j = \omega_j - \Omega_s + \frac{\kappa}{N}\sum_{n=1}^{N} \sin(\varphi_n - \varphi_j) + f\sin(\Phi_j - \varphi_j) + \xi_j, \quad (2)$$

where we assume that the independent stochastic variables $\xi_j = \mathrm{Im}(\Xi_j e^{-i\varphi_j})$ are zero-mean and white Gaussian: $\langle \xi_j(t) \rangle = 0$, $\langle \xi_j(t)\xi_k(t') \rangle = 2D\delta(t-t')\delta_{jk}$. Without loss of generality we may take $\Omega_s = 0$. Let us introduce the complex order parameter(the mean field)

$$R = re^{i\psi} = \frac{1}{N}\sum_{n=1}^{N} e^{i\varphi_n}, \quad (3)$$

thus, Eq. (2) becomes

$$\dot{\varphi}_j = \omega_j + \kappa r \sin(\psi - \varphi_j) + f\sin(\Phi_j - \varphi_j) + \xi_j. \quad (4)$$

Equivalently, it can be written in terms of the complex mean field R (3),

$$\dot{\varphi}_j = \omega_j + \kappa\, \mathrm{Im}[Re^{-i\varphi_j}] + f\sin(\Phi_j - \varphi_j) + \xi_j(t). \quad (5)$$

IV. NOISE-FREE DYNAMICS

In this section we discuss the properties of the driven system (4) without noise. It can be rewritten in a more compact form

$$\dot{\varphi}_j = \omega_j + A_j \sin(\phi_j - \varphi_j) \quad (6)$$

with $A_j = \sqrt{\kappa^2 r^2 + f^2 + 2\kappa r f \cos(\psi - \Phi_j)}$ and $\tan(\phi_j - \Phi_j) = \kappa r \sin(\psi - \Phi_j)/[\kappa r \cos(\psi - \Phi_j) + f]$. The case when all $\Phi_j = 0$ (all oscillators are driven in-phase) was studied by Sakaguchi [5]. He found that, depending on the relative magnitude of driving strength f and coupling constant κ, there can be two distinct regimes: a forced-entrainment regime and a mutual-entrainment regime. In the first case, all oscillators can be divided into two groups: one is synchronized to the driving force and the other remains unsynchronized. In this case for the limit of large N, the order parameter is stationary (in the reference frame rotating with the driving frequency). In the mutual-entrainment regime there are three groups of oscillators: one group is synchronized to the driving force, another group is mutually entrained, and a third group remains unsynchronized. In this case the order parameter is oscillating. Similar dynamics are observed in the general case $\Phi_j \neq 0$.

Let us consider the forced-entrainment regime in the large N limit, so we take r, ψ, A_j, and Ψ_j to be constant. Then Eq. (6) describes standard oscillator phase locking. Depending on the natural frequency, an oscillator is either locked, if $|\omega_j| < A_j$, or drifting, if $|\omega_j| > A_j$.

Locked oscillators have fixed phases

$$\varphi_j = \phi_j + \arcsin(\omega_j / A_j), \quad (7)$$

and drifting oscillators have running phases

$$\varphi_j = \phi_j + \tilde{\omega}_j t + h(\tilde{\omega}_j t), \quad (8)$$

where $\tilde{\omega}_j = \sqrt{\omega_j^2 - A_j^2}$ and $h(x)$ is a 2π-periodic function of x.

We assume that the distribution of oscillators' natural frequencies $g(\omega)$ is independent of the distribution of the driving phases $H(\Phi)$. Note that for an oblique plane wave $H(\Phi)=\Phi_0^{-1}$ within the interval $(0,\Phi_0)$ and zero otherwise with $\Phi_0 = N\Delta\Phi$. The continuum analog of Eq. (3) is

$$re^{i\psi} = \int_0^{2\pi} d\varphi n(\varphi) e^{i\varphi}, \quad (9)$$

where $n(\varphi)$ is the oscillators' phase distribution. Following Ref. [4] we calculate $n(\varphi)$ using Eqs. (7) and (8) as a sum of two contributions, from locked oscillators

$$n^l(\varphi) = \int_{-\infty}^{\infty} d\Phi H(\Phi) A g(A \sin(\varphi - \phi_*)) \cos(\varphi - \phi_*) \theta(\varphi - \phi_*) \quad (10)$$

and from drifting or desynchronized oscillators

$$n^{ds}(\varphi) = \frac{1}{2\pi} \int_{-\infty}^{\infty} d\Phi H(\Phi) \int_{|\omega|>A} d\omega g(\omega) \frac{\sqrt{\omega^2 - A^2}}{\omega - A \sin(\varphi - \phi_*)}. \quad (11)$$

Here $A=\sqrt{\kappa^2 r^2 + f^2 + 2\kappa r f \cos(\psi - \Phi)}$, $\tan(\phi_* - \Phi) = \kappa r \sin(\psi - \Phi)/[\kappa r \cos(\psi - \Phi) + f]$, and $\theta(x)=1$ for $0 < x < \pi/2$ and zero otherwise.

Substituting (10) and (11) into Eq. (9), we get the self-consistency equation for the order parameter

$$re^{i\psi} = \int_{-\infty}^{\infty} d\Phi H(\Phi) B(A) e^{i\phi_*} \quad (12)$$

with

$$B(A) = \int_{-A}^{A} d\omega \left(i\frac{\omega}{A} + \sqrt{1 - \frac{\omega^2}{A^2}} \right) g(\omega) + i \int_A^{\infty} d\omega \left(\frac{\omega}{A} - \sqrt{\frac{\omega^2}{A^2} - 1} \right) [g(\omega) - g(-\omega)]. \quad (13)$$

This complex equation defines the values of r and ψ However, it is difficult to solve this equation in the general case.

Let us first consider the case of decoupled oscillators $\kappa = 0$. Then $A=f$, $\phi_* = \Phi$, and R drops out of the right-hand side of Eq. (12), so we can calculate the mean field explicitly as

$$r_0 e^{i\psi_0} = B(f) Z e^{i\Gamma}, \quad (14)$$

where Z and Γ, real, are given by

$$Ze^{i\Gamma} \equiv \int_{-\infty}^{\infty} d\Phi H(\Phi) e^{i\Phi}. \quad (15)$$

For the uniform phase distribution $H(\Phi)=\Phi_0^{-1}$ within the interval $0 < \Phi < \Phi_0$, the last formula simplifies to $Z = 2\Phi_0^{-1} \sin(\Phi_0/2)$ and $\Gamma = \Phi_0/2$. The magnitude of the mean field depends on the driving amplitude in a nontrivial manner, as the latter determines the relative contribution of the locked and drifting oscillators. For a monochromatic frequency distribution $g(\omega)=\delta(\omega-\omega_0)$, either all oscillators are locked (if $f > \omega_0$) or drifting otherwise. In the locked case, the second term in $B(f)$ is zero, and we get $B(f)=[i\omega_0 + \sqrt{f^2 - \omega_0^2}]/f$, so $r_0 = Z(\Phi_0)$, $\psi_0 = \Phi_0/2 + \arcsin(\omega_0/f)$. In the drifting case, the first term in (13) is zero, and we get $B(f) = i[\omega_0 - \sqrt{\omega_0^2 - f^2}]/f$, so $r_0 = Z(\Phi_0)|B(f)|$, $\psi_0 = \Phi_0/2 + \pi/2$.

For small nonzero κ we look for a solution of the form $r = r_0 + \kappa r_1 + O(\kappa^2)$, $\psi = \psi_0 + \kappa\psi_1 + O(\kappa^2)$, where r_0, ψ_0 are solutions for the uncoupled oscillators, and approximate $A \approx f + \kappa r_0 \cos(\psi_0 - \Phi)$, $\phi_* = \Phi + \kappa r_0 f^{-1} \sin(\psi_0 - \Phi)$. The first-order corrections r_1, ψ_1 can be found from

$$r_1 + i\psi_1 r_0 = r_0 e^{-i\psi_0} \left[B'(f) \int_{-\infty}^{\infty} d\Phi H(\Phi) e^{i\Phi} \cos(\psi_0 - \Phi) + iB(f) f^{-1} \int_{-\infty}^{\infty} d\Phi H(\Phi) e^{i\Phi} \sin(\psi_0 - \Phi) \right]. \quad (16)$$

For large Φ_0 in synchronized case $f > \omega_0$, the first-order correction to the mean-field magnitude is given by

$$r_1 \approx \frac{Z(\Phi_0)}{2\sqrt{f^2 - \omega_0^2}}. \quad (17)$$

In the limit of strong coupling ($\kappa \gg 1$) all oscillators are phase locked near the average phase $\theta(t) = \Sigma_{j=1}^N \varphi_j$. Summing up all phase equations (4), we get

$$\dot{\theta} = \overline{\omega} + \frac{f}{N} \sum_{j=1}^{N} \sin(\Phi_j - \theta - \delta\varphi_j), \quad (18)$$

where $\overline{\omega} = \Sigma_{j=1}^N \underline{\omega_j}/N$ is the mean frequency of the oscillators and $\delta\varphi_j = \varphi_j - \psi$ are (small) deviations of the individual phases from the mean. Neglecting $\delta\varphi_j$, we get the closed equation for the average phase

$$\dot{\theta} = \overline{\omega} + \frac{f}{N} \sum_{j=1}^{N} \sin(\Phi_j - \theta), \quad (19)$$

or in the continuum limit $N \gg 1$,

$$\dot{\theta} = \overline{\omega} + f \int_{-\infty}^{\infty} d\Phi H(\Phi) \sin(\Phi - \theta). \quad (20)$$

This equation can be rewritten in the simpler form

$$\dot{\theta} = \overline{\omega} + fZ \sin(\Gamma - \theta). \quad (21)$$

The oscillators are locked to the driving signal if $\overline{\omega} < fZ$ and drifting otherwise. In the locked regime, the mean field is constant with amplitude $r_l = 1$. In the drifting regime, the mean field oscillates with respect to the driving signal and the response at the "driving frequency" (in our case $\Omega_s = 0$, at zero frequency) can be found as the time average $\langle e^{i\theta} \rangle$

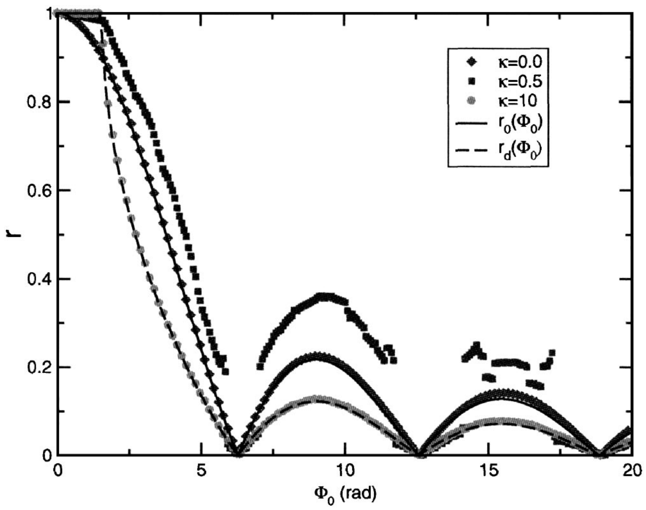

FIG. 3. Mean-field magnitude r as a function of Φ_0 in the absence of noise for $N=10$, $f=1$, $\omega=0.9$ and three different values of coupling $\kappa=0,0.5,10$. Lines correspond to theoretical formulas (14) and (23).

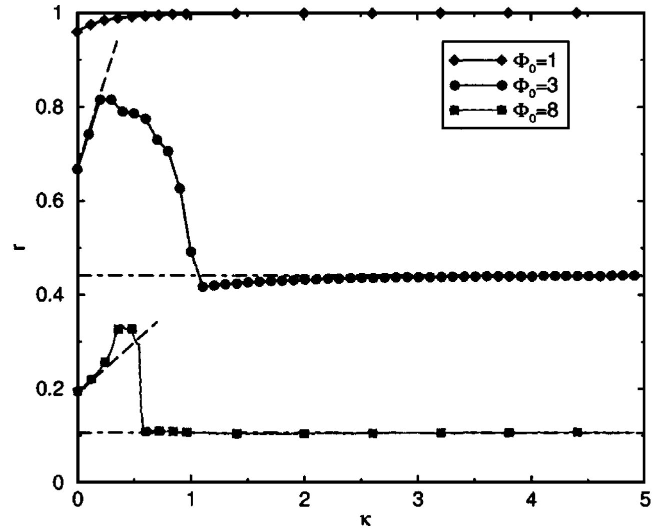

FIG. 4. Mean-field magnitude r as a function of coupling strength κ in the absence of noise for $N=10$, $f=1$, $\omega=0.9$, and three different values of $\Phi_0=1,3,8$.

$$\langle e^{i\theta}\rangle = \frac{\int_0^{2\pi} e^{i\theta}\dot{\theta}^{-1}d\theta}{\int_0^{2\pi}\dot{\theta}^{-1}d\theta}. \tag{22}$$

Performing the integration we obtain the amplitude of the mean field,

$$r_d(\Phi_0) \equiv |\langle e^{i\theta}\rangle| = \frac{\overline{\omega} - \sqrt{\overline{\omega^2} - f^2G^2}}{fG}. \tag{23}$$

Figure 3 show the beam patterns corresponding to the cases of weak coupling [$\kappa=0$, Eq. (14)] and strong coupling [$\kappa \gg 1$, Eq. (23)] for $f=1$ and a monodispersive frequency distribution with $\omega_0=0.9$. The plot also shows numerically calculated beam patterns for $\kappa=0,10$, and an intermediate value of $\kappa=0.5$.

The role of the small $O(\kappa)$ correction (16) is illustrated by Fig. 4, where the mean field dependence on κ is shown for three different directions. The numerical results for $N=10$ are compared with analytical formula (16). As seen from this figure, small coupling leads to an increase of the mean field. Within the region of synchronization $Z(\Phi_0)>\omega_0/f$, this trend continues for all κ and eventually $r\to 1$ as $\kappa\to\infty$. However, outside of the synchronized region, for stronger coupling strength the trend is reversed and the mean field decreases toward the strong-coupling limit (23).

V. FOKKER-PLANCK DESCRIPTION OF MANY NOISY COUPLED OSCILLATORS ($N \gg 1$)

Now let us return to the case of noisy dynamics [$\xi_i \neq 0$ in Eq. (4)]. For large N, the mean field R is not fluctuating and becomes a deterministic function. Then we can introduce the single-oscillator probability distribution function $W_j(\varphi,t) \equiv W(\varphi,t;\omega_j,\Phi_j)=\langle \varphi-\varphi_j(t)\rangle$ and write a Fokker-Planck equation for $W_j(\varphi,t)$

$$\frac{\partial W_j}{\partial t} = -\frac{\partial}{\partial\varphi}[F_j(\varphi)W_j] + D\frac{\partial^2 W}{\partial\varphi^2}, \tag{24}$$

where $F_j(\varphi)=\omega_j+\kappa r\sin(\psi-\varphi)+f\sin(\Phi_j-\varphi)=\omega_j+A_j \times\sin(\phi_j-\varphi)$, $A_j=\sqrt{\kappa^2r^2+f^2+2\kappa rf\cos(\psi-\Phi_j)}$, and $\phi_j=\arctan[\kappa r\sin(\psi-\Phi_j)/\kappa r\cos(\psi-\Phi_j)+f]$. The "phase drift velocity" $F_j(\varphi)$ is a 2π-periodic function of φ.

The stationary solution of Eq. (24) satisfying the periodic boundary condition $W_j(\varphi)=W_j(\varphi+2\pi)$ is given by (cf. [5,15])

$$W_j(\varphi) = \exp\left(\frac{\omega_j\varphi + f\cos(\varphi-\Phi_j) + \kappa r\cos(\varphi-\psi) - \kappa r\cos\psi - f\cos\Phi_j}{D}\right) \times\left\{1 + \frac{(e^{-2\pi\omega_j/D}-1)\int_0^{\varphi} e^{[-\omega_j\tilde{\varphi}-\kappa r\cos(\tilde{\varphi}-\psi)-f\cos(\Phi_j-\tilde{\varphi})]/D}d\tilde{\varphi}}{\int_0^{2\pi} e^{[-\omega_j\tilde{\varphi}-\kappa r\cos(\tilde{\varphi}-\psi)-f\cos(\Phi_j-\tilde{\varphi})]/D}d\tilde{\varphi}}\right\}W_j(0), \tag{25}$$

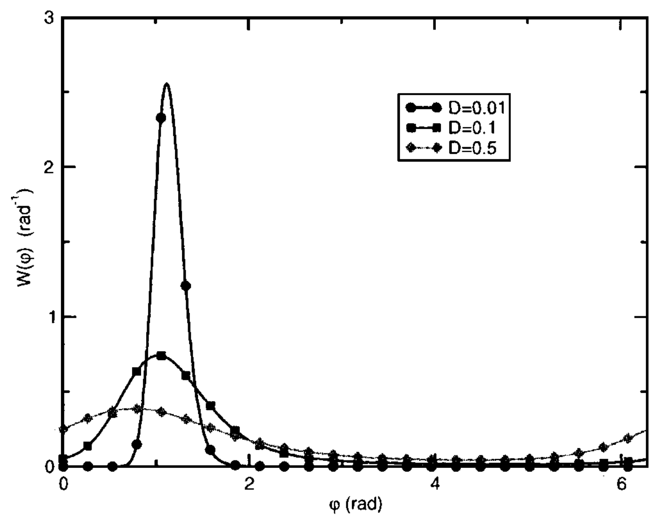

FIG. 5. Phase distributions $W(\phi)$ for $\omega=0.5$, $f=1$, $\kappa=\Delta\Phi=0$, and three different values of D

where $W_j(0)$ is determined by the normalization condition

$$\int_0^{2\pi} W_j(\varphi)d\varphi = 1. \quad (26)$$

Examples of the pair distribution function (PDF) distributions for $\kappa=\Delta\Phi=0$ and various levels of noise D are shown in Fig. 5.

The mean field R can be calculated as

$$R = \frac{1}{N}\sum_{n=1}^{N}\int W_n(\varphi)e^{i\varphi}d\varphi. \quad (27)$$

For large N we can replace the sum by the integration over the frequency and driving phase (Φ) distributions,

$$R = \int_{-\infty}^{\infty} g(\omega)d\omega\int_{-\infty}^{\infty}H(\Phi)d\Phi\int_0^{2\pi}d\varphi W(\varphi;\omega,\Phi)e^{i\varphi}. \quad (28)$$

This complex integral equation must be solved numerically to obtain R.

A. Small noise

Let us consider the case of small D. For locked oscillators ($\omega_j<A_j$), the probability distribution $W_j^l(\varphi)$ is localized near the zeros of $F_j(\varphi)$

$$\varphi_{0j} = \phi_j + \arcsin(\omega_j/A_j). \quad (29)$$

Expanding $F_j(\varphi)=S_j(\varphi-\varphi_{0j})$, where $S_j=\kappa r\cos(\psi-\varphi_{0j})+f\cos(\Phi_j-\varphi_{0j})$, we get

$$W_j^l(\varphi) = \sqrt{\frac{S_j}{2\pi D}}e^{-S_j(\varphi-\varphi_{0j})^2/2D}. \quad (30)$$

For desynchronized oscillators, for small D the probability distribution can be found as the stationary solution of (24) perturbatively,

$$W_j^{ds}(\varphi) = W_0F^{-1}(1 + DF'(\phi)F^{-2}) + O(D^2), \quad (31)$$

where the normalization constant W_0 is

$$W_0 = \int_0^{2\pi}F^{-1}(\varphi)d\varphi. \quad (32)$$

After integration, we obtain

$$W_j^{ds}(\varphi) = \frac{\sqrt{\omega_j^2 - A_j^2}}{2\pi|\omega_j - A_j\sin(\varphi-\phi_j)|}\times\left(1 + D\frac{A_j\cos(\varphi-\phi_j)}{(\omega_j - A_j\sin(\varphi-\phi_j))^2}\right). \quad (33)$$

The mean field can be found as in Sec. IV by averaging $e^{i\varphi}$ over all oscillators. In the continuum limit,

$$R = \int_{-\infty}^{\infty}H(\Phi)d\Phi\int_{-\infty}^{\infty}g(\omega)d\omega\int_0^{2\pi}e^{i\varphi}d\varphi \times\left[\int_{-A}^{A}g(\omega)d\omega W^l(\varphi) + \int_{|\omega|>A}g(\omega)d\omega W^{ds}(\varphi)\right], \quad (34)$$

where we have dropped the subscript j enumerating the oscillators. Using Eqs. (30) and (33), we obtain

$$R = \int_{-\infty}^{\infty}H(\Phi)d\Phi[B(A) + DB_1(A) + O(D^2)]e^{i\phi_*} \quad (35)$$

with $B(A)$ given by (13), and

$$B_1(A) = -\int_{-A}^{A}(2S)^{-1}g(\omega)e^{i\arcsin\omega/A}d\omega. \quad (36)$$

Note that to first order in D, the noise correction only comes from the contribution of the synchronized oscillators.

Now we again consider the case of zero coupling $\kappa=0$. In this case $S=\sqrt{f^2-\omega^2}$ and $\varphi_0=\Phi+\arcsin\omega/f$. In this case the integral can be factored as

$$R = [B(f) + DB_1(f)]\int_{-\infty}^{\infty}H(\Phi)e^{i\Phi}d\Phi. \quad (37)$$

The angular dependence of the mean field is given by the same integral as in the no-noise case. For small nonzero coupling $\kappa\ll 1$, neglecting the terms $O(\kappa D)$, the $O(\kappa)$ correction can be taken directly from Eq. (16).

When κ is large, the difference between phases of individual oscillators is small, $\varphi_j=\theta+\kappa^{-1}\tilde{\varphi}_j+O(\kappa^{-2})$, where the "mean phase" $\theta=N^{-1}\sum\varphi_j$. Summing up all phase equations, we get the equation for the mean phase θ,

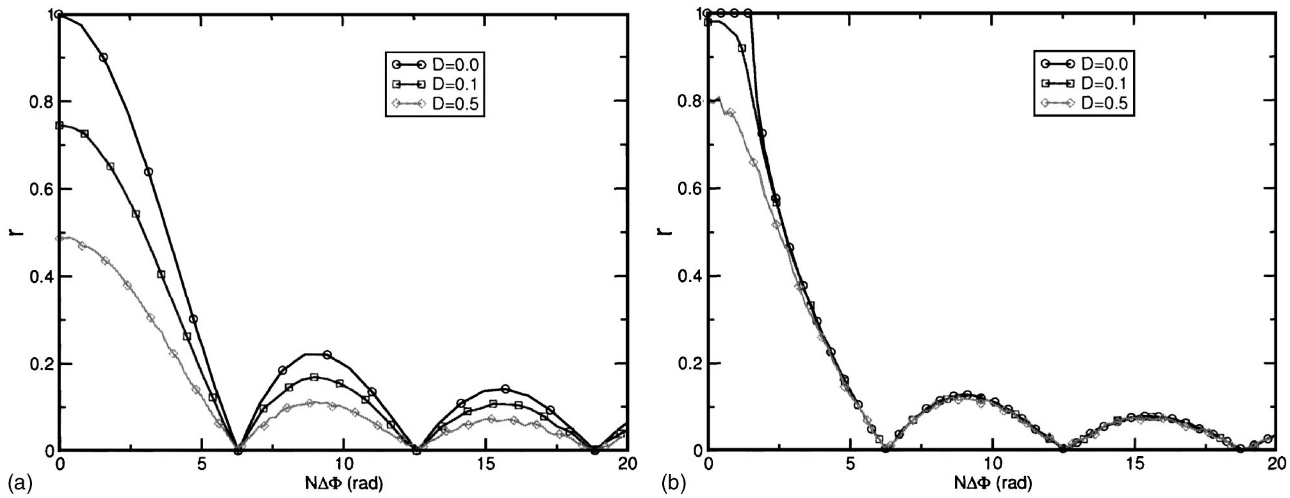

FIG. 6. Beam patterns $r(\Phi_0)$ for different amounts of noise D for the cases of zero coupling $\kappa=0$ (a) and strong coupling $\kappa=10$ (b) for $N=10$, $f=1$, $\omega=0.9$.

$$\dot{\theta}=\overline{\omega}+\frac{f}{N}\sum_{j=1}^{N}\sin(\Phi_j-\varphi_j)+\frac{1}{N}\sum_{j=1}^{N}\xi_j$$
$$=\overline{\omega}+\frac{f}{N}\sum_{j=1}^{N}[\sin(\Phi_j-\theta)+\kappa^{-1}\cos(\Phi_j-\theta)\tilde{\varphi}_j]+\overline{\xi}. \qquad (38)$$

Here $\overline{\xi}$ is the "mean" noise, which has variance D/N and, thus, it disappears in the limit $N\gg 1$. Therefore, in the large-coupling limit for large N one can use noiseless formula (23).

To illustrate the role of noise let us again consider a simple case of identical frequencies $g(\omega)=\delta(\omega-\omega_0)$ and an incident plane incident wave **(**$H(\Phi)=\Phi_0^{-1}$ for $0<\Phi<\Phi_0$**)**. If $f>\omega_0$, then all oscillators are locked and the second term in (13) is absent. In this case the magnitude of the mean field is

$$r=\left(1-\frac{D}{2\sqrt{f^2-\omega_0^2}}\right)\frac{2\sin(\Phi_0/2)}{\Phi_0}+\kappa\frac{\Phi_0-\sin\Phi_0}{2\sqrt{f^2-\omega_0^2}}, \qquad (39)$$

where r_1 is found from (16). As seen from this formula, while the fluctuations tend to reduce the mean-field signal, the small couping always increases the response. For the broadside direction, the last term in Eq. (39) is zero and the higher-order corrections have to be taken into account. However, in fact for $\Phi_0=0$ the mean field can be found for arbitrary κ from the following transcendental equation:

$$r=\exp\left[-\frac{D}{2\sqrt{(f+\kappa r)^2-\omega_0^2)}}\right], \qquad (40)$$

When $1-r\ll 1$, the explicit formula for r reads

$$r=\exp\left[-\frac{D}{2\sqrt{(f+\kappa)^2-\omega^2}}\right]. \qquad (41)$$

In Figs. 6(a) and 6(b) we present the beam patterns for weak and strong coupling at various amounts of noise. Figure 6(a) shows the case of zero coupling $\kappa=0$. In this case increasing noise leads to a uniform decrease of the mean field for all Φ_0. However, for the case of strong coupling [Fig. 6(b)], the effect of noise is strongly suppressed, especially away from the broadside directions.

The comparison between the theory and Monte Carlo simulations for weak ($\kappa=0$) and strong ($\kappa=10$) coupling cases is presented in Fig. 7. The agreement between simulations and (39) is very good throughout the whole range of $N\Phi$. For strong coupling, Eq. (23) agrees with simulations for large $N\Delta\Phi$ away from the broadside direction where the meanfield magnitude is affected by partial synchronization between oscillators and external field.

Figure 8(a) shows the dependence of the mean field r on the coupling strength in Langevin simulations and in theory (39) for a signal incident from the broadside direction.

Figure 8(b) shows the dependence of the mean field r on the coupling strength in Langevin simulations for a larger noise magnitude $D=0.1$ at $\Delta\Phi=0$ (broadside), 0.3, and

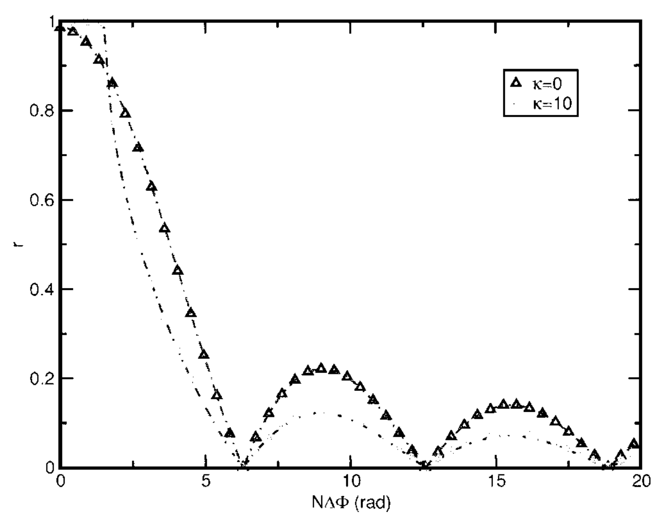

FIG. 7. Mean-field magnitude r as a function of the phase span $N\Delta\Phi$ for $N=10$, $f=1$, $D=0.1$, $\omega=0.9$, and two values of $\kappa=0,10$: comparison between Langevin simulations and theoretical formulas (39) and (23).

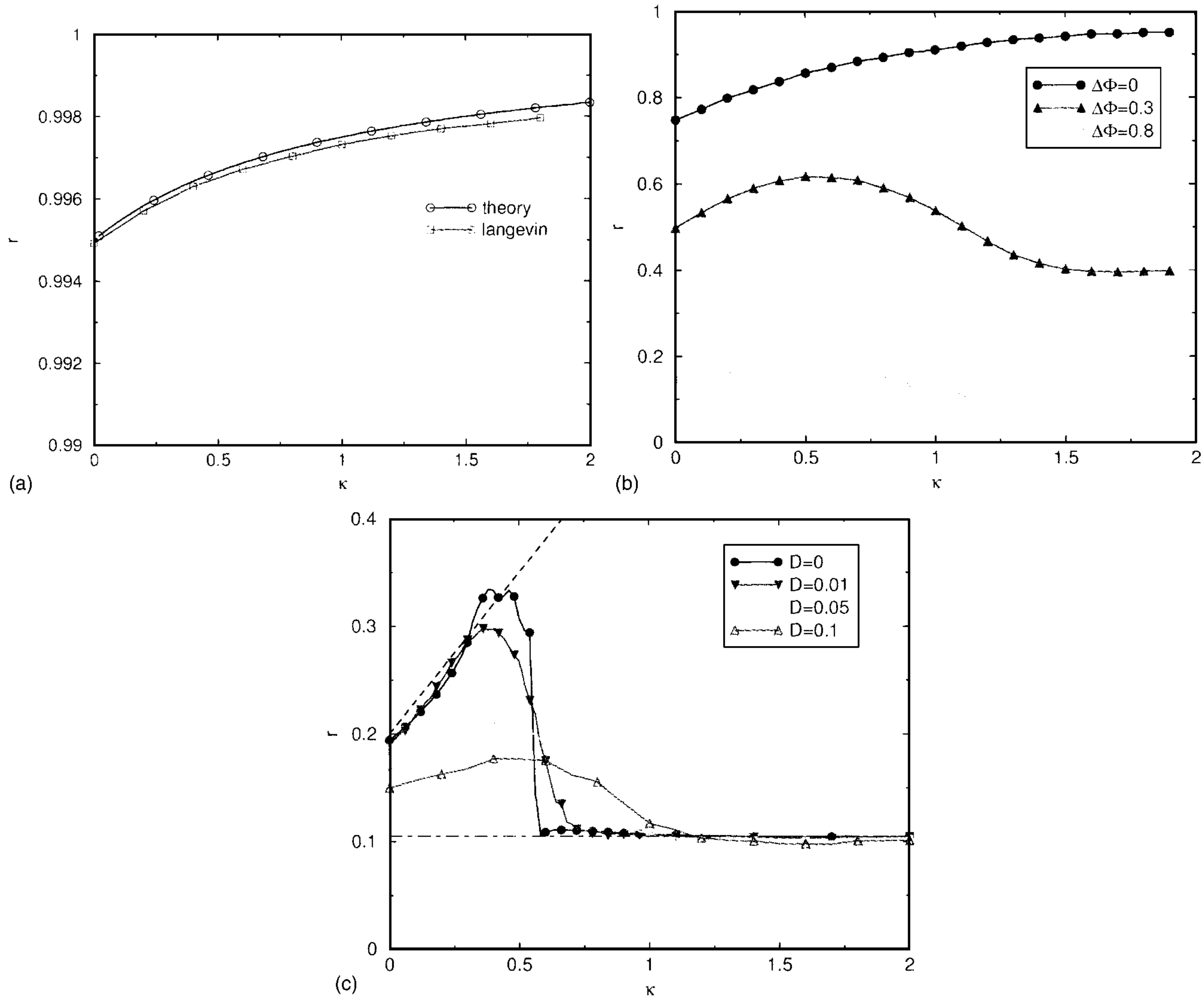

FIG. 8. Mean-field magnitude r as a function of the coupling strength κ for $N=10$, $f=1$, $\omega=0.9$, and small noise $D=0.01$ (a) and stronger noise $D=0.1$ (b). (c) shows the dependence of the mean field on κ for $\Delta\Phi=0.8$ and different values of D. Dashed lines indicate the theoretical dependencies for small κ (39) and large κ (23).

0.8, which corresponds to the first sidelobe. As seen from this figure, in agreement with theoretical analysis, the amplitude of the mean field always increases with κ at small κ, however, away from the broadside it diminishes again at larger κ.

Figure 8(c) shows the dependence of the mean field r on the coupling strength in the Langevin simulations for $\Delta\Phi=0.8$ at different noise magnitudes. In accord with our theoretical analysis, at large κ the mean-field magnitude is insensitive to the noise strength, while at small κ the mean field diminishes with D. The behavior of r for both large and small κ is in good quantitative agreement with theory.

The reason for the growth of the mean field with κ at the broadside direction can be explained as follows. In the phase approximation the coupling parameter κ characterizes the strength of the nonlinearity. For $\kappa\to 0$, the oscillators are decoupled and each of them is driven by its own signal and noise. The outputs of these oscillators are signals $e^{i\varphi_j}$ with phases φ_j independently fluctuating near the same value $\varphi_0=\arcsin(\omega_0/f)$. Averaging the value of $e^{i\varphi_j}$ over phase fluctuations leads to the reduced value of the magnitude of the averaged signal $r\propto\exp(-D/\sqrt{f^2-\omega^2})$. Because the phase fluctuations are not additive, averaging over many oscillators does not eliminate this effect. On the other hand, for large $\kappa\gg 1$, the oscillators are strongly coupled and their phase differences tend to zero. So the whole array acts as a single oscillator with the natural frequency equal to the mean frequency of all oscillators, driven by an average of all incoming signals and noise. Because all incoming signals are identical at the broadside direction, this average is equal to the original input plus the noise, which is reduced by a factor of $N^{1/2}$ due to averaging. Thus, for large N and large κ the magnitude of the output of the array approaches one.

Figure 9 shows the noise dependence of the mean field for different frequencies ω_0 in the absence of coupling. The theoretical formula (39) works well for small $D<0.02$, however, it is rather poor for larger D [Fig. 9(a)]. The range of applicability of the formula shrinks as $\omega\to f$. We also calculated the mean field directly from Eq. (27) for $\kappa=0$, using

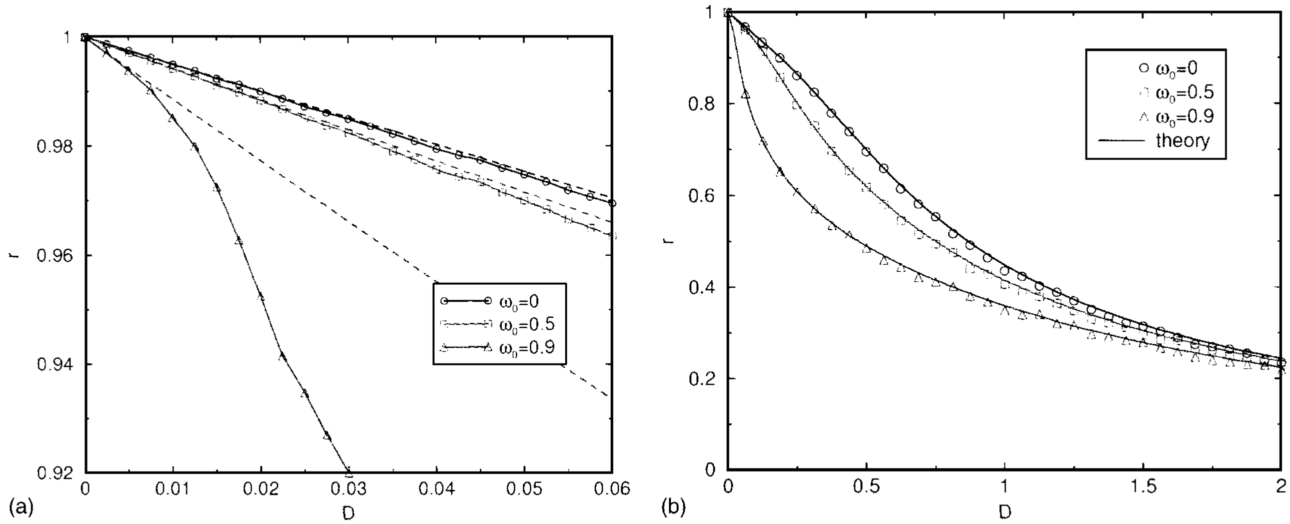

FIG. 9. Mean-field magnitude r as a function of noise strength D for $N=10$, $f=1$, $\Delta\Phi=0$, $\kappa=0$, and three different detuning frequencies ω_0: (a) comparison between the Langevin simulations and Eq. (39) and (b) comparison between simulations and Eq. (27).

numerical integration to obtain the distribution function (25). This theoretical formula is in excellent agreement with the Langevin simulation over the whole range of noise magnitudes [see Fig. 9(b)].

VI. CONCLUSIONS

In this paper we analyzed the properties of a globally coupled array of nonlinear oscillators acting as the beam former of an array receiver antenna. Such a system possesses a number of desirable properties, such as a tunable mainlobe width with a flat shape around the broadside direction and suppressed sidelobes. The mechanism of formation of this unusual beam pattern is related to the synchronization properties of nonlinear oscillators; at and near the broadside direction, the oscillators are synchronized by the external signal, while outside the mainlobe, synchronization is lost, and the oscillators are free-running at their natural frequency.

A number of issues associated with performance of this system have yet to be explored. In particular, because the system is essentially nonlinear, interference with other strong signals (jamming) cannot be described by a single beam diagram and must be analyzed separately. Furthermore, unlike the standard linear beam former, the selection of optimal parameter values for nonlinear oscillators (nonlinear "weights") is far from trivial and no general algorithm exists for that purpose.

ACKNOWLEDGMENT

This work was supported by the Defense Advanced Research Project Agency (N66001–03–C-8049).

[1] K. Wiesenfeld, P. Colet, and S. Strogatz, Phys. Rev. E **57**, 1563 (1998).
[2] Y. Braiman, T. A. B. Kennedy, K. Wiesenfeld, and A. Khibnik, Phys. Rev. A **52**, 1500 (1995).
[3] D. Golomb, D. Hansel, B. Shraiman, and H. Sompolinsky, Phys. Rev. A **43**, 6990 (1990).
[4] Y. Kuramoto, *Chemical Oscillations, Waves, and Turbulence* (Springer, Berlin, 1984).
[5] H. Sakaguchi, Prog. Theor. Phys. **79**, 39 (1988).
[6] H. Daido, J. Stat. Phys. **60**, 753 (1990).
[7] S. H. Strogatz and R. E. Mirollo, J. Stat. Phys. **63**, 613 (1991).
[8] J. D. Crawford, J. Stat. Phys. **74**, 1047 (1994).
[9] H. Hong, M. Y. Choi, K. Park, B.-G. Yoon, and K.-S. Soh, Phys. Rev. E **60**, 4014 (1999).
[10] T. Heath, K. Wiesenfeld, and R. A. York, Int. J. Bifurcation Chaos Appl. Sci. Eng. **10**, 2619 (2000).
[11] M. Gabbay, U.S. Patent No. 20020159335 (October 31, 2002).
[12] M. Gabbay and M. Larsen, Proc. IEEE Aerospace Conf. 3, 1405 (2003).
[13] L. Gammaitoni, P. Hanggi, P. Jung, and F. Marchesoni, Rev. Mod. Phys. **70**, 223 (1998).
[14] P. S. Hagan, SIAM (Soc. Ind. Appl. Math.) J. Appl. Math. **42**, 762 (1982).
[15] R. L. Stratonovich, *Topics in the Theory of Random Noises*, Vol. 2 (Gordon and Breach, New York, 1967).